determined spectrophotometrically at these wave lengths providing sufficient resolution is effected.

Acknowledgment.—The authors express sincere appreciation to the Office of Naval Research and to the Lindsay Light and Chemical Company for the support which rendered this investigation possible.

URBANA, ILL. RECEIVED JANUARY 29, 1951

[CONTRIBUTION FROM THE DEPARTMENT OF CHEMISTRY OF THE UNIVERSITY OF WISCONSIN]

The Structure of Liquid Aluminum Chloride

BY R. L. HARRIS,[1] R. E. WOOD AND H. L. RITTER

A vacuum X-ray camera is described for obtaining diffraction patterns of liquids at high temperatures using crystal monochromatized X-rays. Diffraction patterns for fused aluminum chloride have been obtained and a radial distribution function calculated according to the method of Warren, Krutter and Morningstar. Most of the coherent scattering is due to molecular Al_2Cl_6. The structure of the Al_2Cl_6 molecule in the liquid state is deduced and agrees well with the structure determined by Palmer and Elliott from the electron diffraction of gaseous Al_2Cl_6.

The identity and disposition of the molecular and ionic species present in molten salts is of considerable interest. It would seem that the methods of X-ray diffraction might be made to yield considerable information about the interatomic geometry of such systems. Lark-Horovitz and Miller[2] have published a very brief summary of their work on molten lithium, sodium and potassium chlorides. Quantitative treatment of the molten lithium and potassium salts showed that the coördination scheme and interatomic distances in each were nearly the same as in the corresponding solid. The similarity between the time-average structure of the liquid and the crystal structure of the solid is, of course, restricted to the immediate vicinity of each atom. These two structures were treated in the X-ray analysis as assemblages of single scattering species; the X-ray scattering of Li^+ being taken as negligible in comparison with Cl^-, and the isoelectronic K^+ and Cl^- being taken as identical. At that time no method was in use for treating the scattering of X-rays from assemblages of two differently scattering atoms. More recently an attack on such systems has been described by Warren, Krutter and Morningstar[3] and applied with considerable success to vitreous[4] and liquid[5] structures. These latter achievements suggest a means for studying the structure of molten salts in general.

We have applied this technique in particular to liquid aluminum chloride. The properties of this liquid are anomalous in many respects, and one might expect an elucidation of the liquid structure to provide a valuable link in understanding the anomalies. For example, the melting point[6] and molar volume[7] of solid aluminum chloride are abnormally high in comparison to the bromide and iodide, while the molar volume of the liquid chloride is about as expected. There is an unusually large decrease in density (about 45%) on melting. The electrical conductivity of solid aluminum chloride increases in the normal rapid fashion as the melting point is approached but falls abruptly nearly to zero on melting.[7] These facts seem to indicate that aluminum chloride undergoes a fundamental and gross change in structure when it melts. Ketelaar, MacGillavry and Renes[8] have shown the crystal structure of aluminum chloride to be based on an ionic bonding scheme. A change to covalent bonding in the liquid would explain these anomalies. Gerding and Smit[9] found their Raman data on liquid aluminum chloride suggestive of discrete Al_2Cl_6 molecules. Just above the sublimation point, moreover, aluminum chloride vapor has been found to consist of Al_2Cl_6 molecules, both from vapor density measurements[10] and by electron diffraction.[11] The fact that the Trouton constant for fused aluminum chloride is normal[12] strongly suggests that the liquid also consists of discrete Al_2Cl_6 molecules. The present research confirms this supposition.

Experimental

The camera (Fig. 1) is designed for obtaining photographic records of diffraction patterns up to Bragg angles of about 85° and up to temperatures of about 900°. The tripod mount A has its plane inclined 6° below the horizontal and rotates about the vertical post B. The axis of rotation coincides with that of the holder C for the crystal monochromator. The cylindrical camera of 57.3 mm. radius carries a collimator D with pinholes 1 mm. in diameter spaced 50 mm. apart. A beam trap E helps to cut down air scattering and is fitted with a fluorescent screen backed with lead glass. The assembly carrying the heater and sample holder is supported from the camera cover. The latter is removable and joins the camera body through a gasketed seal F which permits operation in a vacuum or inert gas. The heating element is constructed by winding helically on a Lavite core G a tight helix of No. 26 nichrome wire (20 ohms). The heater is surrounded by a heavy Lavite insulator, K, and the whole assembly enclosed in a brass can, L. Cooling water is circulated through $^1/_4$″ copper tubing soldered to the outside of the can as well as to the sides and bottom of the camera body. The electrical lead to the heater is passed through a Kovar and glass tube in the lid, H. The temperature is regulated by Variac and measured by a chromel–alumel thermocouple whose junction is placed close to the sample. A monel cylinder I is placed within the heater core and carries a threaded fitting in the bottom.

(1) Allied Chemical and Dye Corporation, Morristown, N. J.

(2) K. Lark-Horovitz and E. P. Miller, *Phys. Rev.*, **49**, 418 (1936).

(3) B. E. Warren, H. Krutter and O. Morningstar, *J. Am. Ceram. Soc.*, **19**, 202 (1936).

(4) See, for example, B. E. Warren, *Chem. Revs.*, **26**, 237 (1940).

(5) See, for example, E. E. Bray and N. S. Gingrich, *J. Chem. Phys.*, **11**, 351 (1943).

(6) W. Biltz, *Z. anorg. Chem.*, **121**, 257 (1922).

(7) W. Biltz and A. Voigt, *ibid.*, **126**, 39 (1923).

(8) J. A. A. Ketelaar, C. H. MacGillavry and P. A. Renes, *Rec. trav. chim.*, **66**, 501 (1947).

(9) H. Gerding and E. Smit, *Z. physik. Chem.*, **B50**, 171 (1941).

(10) H. Deville and L. Troast, *Compt. rend.*, **45**, 821 (1857).

(11) K. J. Palmer and N. Elliott, THIS JOURNAL, **60**, 1852 (1938).

(12) A. Smits, J. L. Meijering, M. A. Kamermans, *Proc. Acad. Sci. (Amsterdam)*, **34**, 1327 (1931); A. Smits and J. L. Meijering, *Z. physik. Chem.*, **B41**, 98 (1938).

A small hole in this fitting holds and centers the sample tube in the collimated X-ray beam. The 35 mm. film is covered with black paper if necessary and held against the inner cylindrical surface of the camera by retaining rings. A nipple M serves to evacuate the camera or to fill it with inert gas.

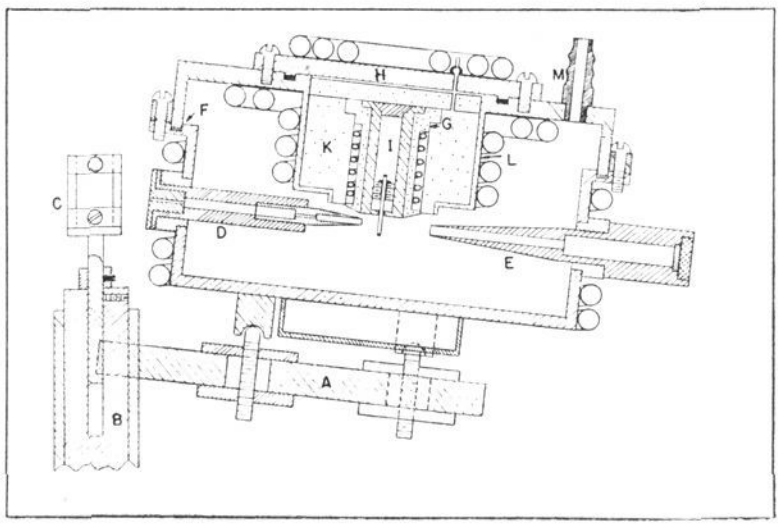

Fig. 1.—High temperature X-ray camera for liquid samples.

The monochromating crystal is urea nitrate. Lonsdale[13] has pointed out that this substance produces strong reflections from the 002 planes, which are well-developed faces as well as cleavage planes. The interplanar spacing also is such as to give a useful separation of the primary and monochromated beams. A further marked advantage of urea nitrate as a monochromator is the relatively low intensity of the 004 reflection—about one-sixtieth that of the 002. Thus when the crystal is set to select from a heterochromatic beam a desired component of wave length λ reflected from 002, it will also select $\lambda/2$ reflected from 004. The intensity of $\lambda/2$ however will be reduced one-sixtieth as much as λ. If characteristic radiation is chosen for λ, the favorable factor of 60 is in addition to the normal relative intensities of the characteristic radiation and of the half wave length occurring in the white radiation. Since this latter factor is usually quite high, the combined factors make it possible to excite the X-ray tube well above the excitation potential for $\lambda/2$, without sacrificing monochromaticity of the beam so far as its $\lambda/2$ content is concerned.

The sample was enclosed in a glass capillary tube under partial vacuum and sealed at both ends. Because of the high vapor pressure of liquid aluminum chloride it was found necessary to enclose it in a tube unusually thick for X-ray work. The uniform tube chosen for the final photographs was 0.41 mm. inside diameter with walls 0.13 mm. thick. Since the diffraction pattern produced under these circumstances has a large contribution due to diffraction by the glass, the glass pattern must be subtracted from the total. Accordingly, exposures under the same total X-ray flux were made of the capillary both filled and empty. It should be noted that it is not permissible simply to subtract the pattern due to the glass tube alone from the total pattern. The blank pattern is affected only by self-absorption while the glass-contribution to the total pattern is affected by absorption in the sample as well. Thus the contribution of the glass to the total pattern is not identical with the pattern of the glass alone. A method for handling this correction as well as the other absorption corrections involved in a compound sample is described elsewhere.[14]

Pairs of exposures were made of sample and blank and developed under identical conditions. The exposures lasted 200 hours and the X-ray intensity from the monochromator was checked before, during and after each exposure to ensure equal integrated X-ray flux. The temperature of the liquid aluminum chloride was 220 ± 5°. The films were microphotometered and microphotometer readings converted to intensity in the usual way.

Calculations

The observed intensities were corrected for glass diffraction, absorption and polarization. The resulting intensities are on an arbitrary scale. This scale was made absolute by fitting the corrected-observed intensities to the calculated scattering for independent atoms at large values of $s = (4\pi/\lambda) \sin(\theta/2)$, where θ is the diffraction angle. The calculated independent scattering curve, both coherent and incoherent, is based on the stoichiometric unit $AlCl_3$. Figure 2 (lower part) shows this curve, computed as $\Sigma f_{coh}^2 + \Sigma f_{inc}$, where the summation is extended over one $AlCl_3$ unit and f_{coh} and f_{inc} are, respectively, the coherent and incoherent atomic structure factors. Superposed on this curve is the experimental corrected curve, with its vertical scale adjusted to make it coincide at the largest reliable s with the independent scattering. Also shown is the calculated incoherent scattering.

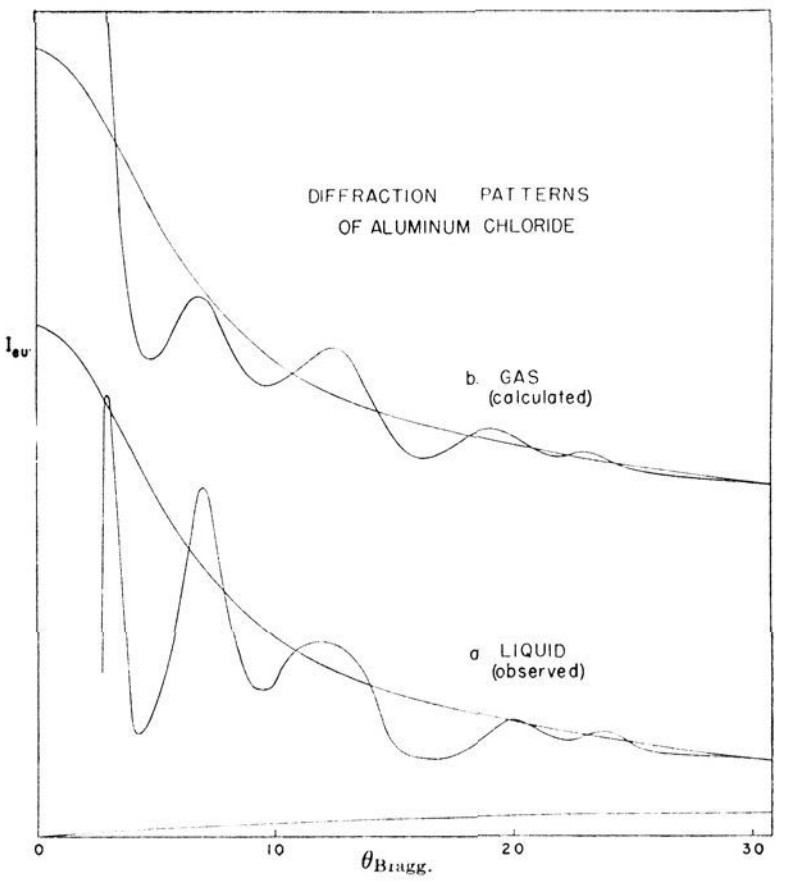

Fig. 2.—Observed and calculated diffraction patterns for liquid aluminum chloride. In the lower part of the figure, the monotonic decreasing curve is the calculated independent atomic scattering for $AlCl_3$, the monotonic increasing curve is the incoherent part alone, and the oscillating curve is the corrected and fitted observed scattering. The upper part of the figure shows the calculated scattering for independent Al_2Cl_6 molecules.

The incoherent scattering is now subtracted from the other two curves in Fig. 2, obtaining: I_{cor} = the experimental intensity corrected for absorption and polarization as well as for incoherent scattering, and reduced to absolute units; and Σf_{coh}^2, the coherent scattering for the independent atoms in the same units. We then define a new function of s

$$i(s) = \frac{I_{cor}}{\Sigma f_{coh}^2} - 1$$

It has been shown[3] that the radial distribution of electron density surrounding any chosen atom in an arbitrary collection of atoms is given by the expression

(13) K. Lonsdale, *Proc. Roy. Soc.* (*London*), **A177**, 272(1941).

(14) H. L. Ritter, R. L. Harris and R. E. Wood, *J. App. Physics*, **22**, 169 (1951).

$$4\pi r^2 \sum_m K_m g_m = 4\pi r^2 g_0 \sum_m K_m + \sum_m K_m^2 \, 2r/\pi \int_0^\infty si(s) \sin rs \, ds \quad (1)$$

where

r is the radial distance from any atom, m
g_m is the r-dependent electron density (electrons/Å.^{3}) in the matter surrounding atom m
$4\pi r^2 g_m dr$ is the number of electrons contained in a spherical shell of radii r and $r + dr$ drawn about atom m
K_m is an effective atomic number of atom m
Σ extends over the unit of composition ($AlCl_3$)
g_0 is the *average* (independent of r) electron density of the matter

The first term on the right evidently represents the product of (the average number of electrons at distance r) multiplied by (the total effective number of electrons in one $AlCl_3$ unit). The term on the left is the corresponding r-dependent function. It is a weighted density function representing the sum, over all the atoms of the unit composition, of the product of (the effective number of electrons in a chosen atom) multiplied by (the r-dependent electron density of the matter surrounding that atom). The first term on the right is a parabola, and alone would indicate in the radial distribution no preferred distances between atoms. The second term on the right modifies this "homogeneous" average by adding or subtracting the excess or deficiency of electron density corresponding to these preferred distances. A plot of r *vs.* $4\pi r^2 \Sigma K_m g_m$ will show peaks at values of r corresponding to popular interatomic distances and valleys at unlikely ones. This plot is really the superposition of two radial distribution curves; one for the distribution around an Al atom and one for the distribution around a Cl atom.

The evaluation of this weighted density function involves then the evaluation of the right-hand side of equation (1). The term g_0 may be calculated directly from the density of liquid $AlCl_3$ (taken as 1.26 g./cc.),[7] and other fundamental constants. The value used here was $g_0 = 0.364$ electron/Å.^{3}. K_m, the "effective" atomic number, may be obtained from the relation

$$K_m = f_m \frac{\Sigma Z_m}{\Sigma f_m}$$

where f_m is the ordinary coherent atomic structure factor for atom m. Since f_m is a function of s, K_m is also a function of s. The values of K_{Al} and K_{Cl} do not vary greatly over the range of s values used, however, and replacing the variable $K_m(s)$ by a constant average K_m is feasible. The values chosen were $K_{Al} = 12.3$ and $K_{Cl} = 17.3$.

The integral on the right of the equation (1) must be evaluated numerically at enough values of r to define the distribution curve sufficiently well. It is convenient to divide the integrand into two factors: $si(s)$ and sin rs. The former of these is plotted in Fig. 3. The authors effected the integration by means of the trapezoidal rule, the specific adaptation of which seems sufficiently novel and labor-saving to justify a brief description.

It will be seen from Fig. 3 that the practical limits of the integral are $s = 0$ and $s = 8.72$. At both

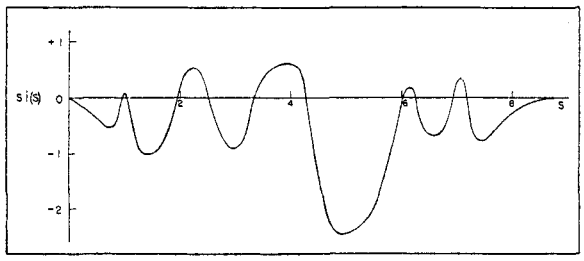

Fig. 3.—The function $si(s)$ *vs.* s for liquid aluminum chloride.

these points the integrand vanishes. The trapezoidal rule then reduces to

$$\int_0^{8.72} si(s) \sin rs \, ds = \Delta s \sum_0^{8.72} si(s) \sin rs$$

where the summend is evaluated at equispaced intervals between the limits. Accordingly, the function $si(s)$ is reduced to tabular form in increments of say $\Delta s = 0.02$. The summation now requires the value of the products $si(s)$ sin rs for every tabulated value of s—some 430 values. This means working out the 430 values of rs and looking up their sines. If however r is so chosen that $rs_i = 2\pi$ when s_i is some (low) *tabulated* value, then sin rs_i, sin $r2s_i$, sin $r3s_i$, etc. all vanish and intermediate values repeat in cycles. For example, if $r = 5.0671$, then rs is a multiple of 2π when $s = 0$, 1.24, 2.48, . . ., 8.68, all of which are tabulated. The range of s values is covered with seven sine cycles, so that only one-seventh of the tabulated s's must be individually converted to sin rs. Moreover, because of the antisymmetry of the sine function, half of these values are simply the negative of the other half and need not be looked up. Furthermore, even one loop of the sine curve is symmetrical about its maximum, and only half the loop need be looked up. Thus for giving up the "convenience" of evaluating the integral at $r = 5$ and accepting the unrounded value of $r = 5.07$ instead, one gains the advantage of having to enter the sine tables only some 15 times instead of 430. Less extensive tables are consequently required also. In addition, all those values of $si(s)$ for which sin rs are equal can be combined and evaluated as sin rs $\Sigma_{\pm} si(s)$, thus effecting a large saving in not having to compute individually the products $si(s)$ sin rs. In actual practice, it is simple to prepare tabular forms that make the trapezoidal calculation automatic and as much as ten times as fast as evaluation at an arbitrary r. Since it is the sketching of the whole curve $4\pi r^2 \Sigma K_m g_m$ *vs.* r that is required rather than the value of $4\pi r^2 \Sigma \cdot K_m g_m$ at particular values of r, it serves just as well to use unrounded values of r as rounded ones. With the cycle pattern prepared, an integration for one value of r may be completed in about one man-hour's time.

Results

Equation (1) was evaluated at 57 points, and the resulting distribution curve is plotted in Fig. 4. The parabolic curve in this figure is the mean distribution given by the first term on the right of equation (1). Peaks are evident at $r = 2.20$, 3.60, 4.74, 5.57 and 6.52 Å. These values of r correspond to interatomic distances which repeat predomi-

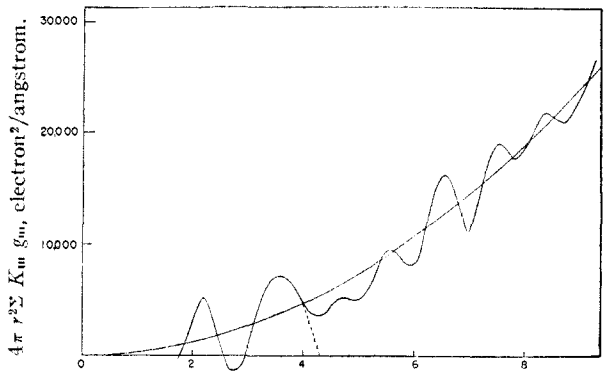

Fig. 4.—Radial distribution curve for liquid aluminum chloride.

nantly in the liquid. The ratio of the first two r's, $3.60/2.20 = 1.636$, is very nearly $\sqrt{8/3} = 1.633$, the ratio of the length of an edge of a regular tetrahedron to its center-to-apex distance. This fact strongly suggests a structure based on tetrahedral coördination of Cl atoms around an Al atom. The model of Palmer and Elliott[11] consists of Al_2Cl_6 molecules in which the six Cl atoms are at the apices of a shared-edge double tetrahedron with one Al atom in each tetrahedron. This scheme is pictured in Fig. 5, where the small black dots represent Al atoms and the larger open circles Cl atoms. The two tetrahedra are formed by Cl atoms 5678 and 5438, 58 being the common edge.

Comparison of the observed r values with those that would be exhibited by a *regular* double tetrahedron indicates that the Al_2Cl_6 molecule is considerably distorted from this form. In a regular figure, distances 6-4 and 6-3 are, respectively, 5.09 and 6.24, based on a tetrahedral edge of 3.60. Since these are the longest interatomic distances within the molecule, it is reasonable to identify the real distances 6-4 and 6-3 with the observed r values of 5.57 and 6.52. This assignment of the 5.57 and 6.52 peaks requires a stretching of the molecule in the direction of the y-axis, and completely determines the rectangle 3467 in the xy plane of Fig. 5.

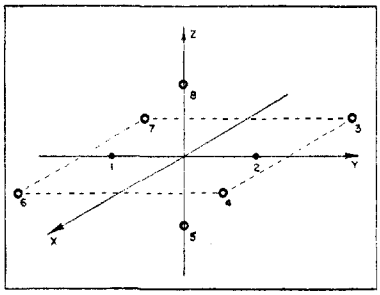

Fig. 5.—Diagram of atomic positions in the Al_2Cl_6 molecule. The numbers correspond to the positions referred to in the text.

The Cl–Cl distance 3-4 is thereby fixed at 3.39, apparently a part of the broad peak at 3.60. The 4.74 Å. peak is identifiable with the Al–Cl distances of the type 1-3. If this distance is taken as 4.74, then the Al–Cl distances of the type 1-6 are fixed at 2.06. There are four such distances lying in the xy plane and four more involving Cl atoms 5 and 8. If it is assumed that the 2.20 peak is made up from these eight distances, half of which are 2.06, it is reasonable to estimate the remaining four distances of the 2–5 type to be about 2.34 Å. This assignment fixes the positions of Cl atoms 5 and 8 and the Cl–Cl distance 5–8 at 3.28 Å. All eight atoms are now fixed. The Al–Al distance 1–2 may be calculated as 3.28 Å. and falls also in the broad peak at 3.60. The Cl–Cl distances of the type 5–6 of which there are eight, are also fixed at 3.65. Thus the 3.60 peak appears to be a fusion of eight Cl–Cl distances of 3.65, one Cl–Cl distance of 3.28, two Cl–Cl distances of 3.39, and one Al–Al distance at 3.28. The weighted average is 3.57, in good agreement with the observed value of 3.60.

Table I shows a summary of the interatomic distances, according to the regular double-tetrahedron, according to Palmer and Elliott for gaseous aluminum chloride, and according to this research. The agreement between the latter two is satisfactory, and indeed probably should not be complete.

TABLE I

INTERATOMIC DISTANCES IN ALUMINUM CHLORIDE

Atoms	Type[a]	Frequency	Regular double tetrahedron	Gaseous[b] Al_2Cl_6	Liquid[c] Al_2Cl_6
Al–Cl	1-6	4	2.20	2.06	2.06
Al–Cl	2-5	4		2.21	2.34
Al–Al	1-2	1	2.53	3.41	3.28
Cl–Cl	5-8	1	3.59	2.83	3.28
Cl–Cl	3-4	2		3.53	3.39
Cl–Cl	5-6	8		3.56	3.65
Al–Cl	1-3	4	4.21	4.77	4.74
Cl–Cl	4-6	2	5.09	5.49	5.57
Cl–Cl	3-6	2	6.24	6.52	6.52

[a] As shown in Figure 5. [b] According to Palmer and Elliott.[11] [c] This research.

Additional confirmation of this model is available from the same distribution curve. The area under this curve, determined between the limits r_1 and r_2, is $\int_{r_1}^{r_2} 4\pi r^2 \Sigma K_m g_m \, dr$. This integral may be rewritten as $\Sigma K_m \int_{r_1}^{r_2} 4\pi r^2 g_m dr$, where $\int_{r_1}^{r_2} 4\pi r^2 g_m dr$ represents the number of electrons that can be counted surrounding atom m and lying between the limits r_1 and r_2. Calling this number N_m, the original integral equals simply $\Sigma K_m N_m$, where the summation is carried over one Al and 3Cl. Thus

$$\text{Area} = K_{Al}N_{Al} + 3K_{Cl}N_{Cl} \qquad (2)$$

Let the limits of integration be chosen such as to include the entire first peak at 2.20 Å. The area will then represent $\Sigma K_m N_m$ where N_m is the number of electrons lying in the immediate coördination sphere around atom m. If the coördination number of Al is n, there are nCl atoms around an Al atom. From the stoichiometry, there must therefore be an average of $n/3$ Al atoms around each Cl atom. In nCl atoms there are nK_{Cl} electrons so that $N_{Al} = nK_{Cl}$. Similarly, $N_{Cl} = nK_{Al}/3$. From equation (2), therefore, the area of the first peak is $2nK_{Al}K_{Cl}$. The measured area under this peak (Fig. 4) is 2030 electron², giving $n = 4.7$

Considering the error normally involved in the process of fitting the observed intensities to the scale of calculated independent scattering at large s, this result can be interpreted as a coördination number of either 4 or 5. In the light of all evidence, the latter possibility is remote.

The second peak at 3.60 Å. in the distribution curve may be treated in the same way. The area will be given by $\Sigma K_m N_m$, where N_m now represents the number of electrons lying at about 3.6 Å. from atom m. From Table I, the Al–Al distance, 1–2, and the three Cl–Cl distances, 5–8, 3–4 and 5–6, all lie within this peak. There are one such Al–Al distance and eleven such Cl–Cl distances. Then

$$\text{Area} = K_{Al}^2 + 11K_{Cl}^2 = 3470 \text{ electron}^2$$

The measured area (dotted) is 5350 electron^2. The discrepancy is due mostly to *inter*molecular scattering; that is, there appears to be a large contribution to the liquid scattering due to interference between contiguous Cl atoms in neighboring molecules.

Intermolecular Scattering

The first five peaks in the experimental radial distribution curve have been shown to be due largely to intramolecular scattering. This fact suggests that the rather well-defined sixth and seventh peaks are also due to interference between molecules. In an attempt to determine the extent of intermolecular scattering, the data of Table I were entered into the Zernike and Prins formula

$$I_{eu} = \sum_i \sum_j f_i f_j \frac{\sin r_{ij}s}{r_{ij}s} \qquad (3)$$

This expansion would give the pattern to be expected from Al_2Cl_6 molecules diffracting independently. The upper curve in Fig. 2 shows this computed scattering pattern. The general agreement between the patterns is clear, but the influence of intermolecular scattering considerably distorts the experimental curve. An attempt was made to apply the Warren analysis by defining a new $i(s)$

$$i(s) = \frac{I}{I_{mol}} - 1$$

where I_{mol} is a kind of "molecular structure factor," defined by equation (3). Σf_{coh}^2 may be looked upon as given by equation (3) when all the interatomic r_{ij}'s are omitted, and leads through the Warren analysis to the geometric disposition of *atoms* in the mass. Using the whole of I_{mol} expands Σf_{coh}^2 to include the intramolecular geometry, and it was hoped that the Warren analysis might then lead to a geometric disposition of *molecules*. The results were disappointing and yielded no interpretable information.

Integration of the upper curve in Fig. 2 (scattering from independent molecules) in accordance with equation (1) yields a radial distribution curve similar to Fig. 4. In this "synthetic" curve, the positions of the first five peaks are unchanged from Fig. 4, although the shapes of the peaks are different. The sixth and seventh peaks, however, are shifted from their positions in the observed pattern and moreover are almost completely suppressed in the synthetic distribution. These peaks presumably represent distances between atoms in adjacent molecules but they furnish no information about the molecular orientation.

Acknowledgment.—The authors wish to thank both the Wisconsin Alumni Research Foundation and the du Pont Company for grants which made this work possible. Thanks are also due Mr. L. Lincoln for construction of the camera used in the experimental part.

MADISON, WIS. RECEIVED DECEMBER 22, 1950

[CONTRIBUTION FROM THE MULTIPLE FELLOWSHIP OF BAUGH AND SONS COMPANY, MELLON INSTITUTE]

The Determination of Pore Volume and Area Distributions in Porous Substances. II. Comparison between Nitrogen Isotherm and Mercury Porosimeter Methods

BY LESLIE G. JOYNER, ELLIOTT P. BARRETT AND RONALD SKOLD

Two of the authors have recently proposed a theory and developed a technique for obtaining pore volume and area distribution data on porous substances from low temperature nitrogen desorption isotherms. To obtain additional evidence as to the validity of this method, pore volume distribution curves were determined for some of the same adsorbents by means of a high pressure mercury porosimeter. Satisfactory agreement between the two methods was obtained. Since the two methods are based on independent principles and techniques this agreement constitutes an excellent confirmation of the proposed theory.

A previous publication[1] has described a method for obtaining the pore volume and area distribution of porous substances with respect to pore radius from the desorption branch of the low temperature nitrogen isotherm. The method took into consideration desorption from multilayers as well as Kelvin evaporation from capillaries. In that paper it was shown that for all systems examined the total area obtained from the distribution data was in substantial agreement with the total area as determined by the BET method.[2] (This method of obtaining the distribution curve will be termed the isotherm method.)

A direct method of obtaining pore volume distributions by the use of a high pressure mercury porosimeter has been described by Ritter and Drake.[3] (This method will be termed the porosimeter method.) This method is entirely independent of the adsorption isotherm. Therefore

(1) E. P. Barrett, L. G. Joyner and P. P. Halenda, THIS JOURNAL, **73**, 373 (1951).

(2) S. Brunauer, P. H. Emmett and E. Teller, *ibid.*, **60**, 309 (1938).

(3) H. L. Ritter and L. C. Drake, *Ind. Eng. Chem. Anal. Ed.*, **17**, 782 (1945).